


Algorithms to improve unmanned aerial vehicle positioning accuracy using European Geostationary Navigation Overlay Service and System for Differential Corrections and Monitoring ionospheric corrections

Kamil Krasuski^{1*} , Mieczysław Bakuła¹, Paweł Gołda², Adam Ciećko³,
Grzegorz Grunwald³, Magda Mrozik⁴, Jarosław Kozuba⁴

¹ Institute of Navigation, Polish Air Force University, ul. Dywizjonu 303 nr 35, 08-521 Dęblin, Poland

² Faculty of Aviation, Polish Air Force University, ul. Dywizjonu 303 nr 35, 08-521 Dęblin, Poland

³ Faculty of Geoengineering, University of Warmia and Mazury in Olsztyn, ul. Oczapowskiego 2, 10-720 Olsztyn, Poland

⁴ Faculty of Transport and Aviation Engineering, Silesian University of Technology, ul. Krasińskiego 8, 40-019 Katowice, Poland

* Corresponding author's e-mail: k.krasuski@law.mil.pl

ABSTRACT

This paper presents a modified algorithm for determining the positioning accuracy of a unmanned aerial vehicle (UAV) based on a joint Global Positioning System/European Geostationary Navigation Overlay Service + Global Positioning System/System for Differential Corrections and Monitoring (GPS/EGNOS+GPS/SDCM) solution. Firstly, the average weighted model for determining the position of the UAV was developed. The algorithm takes into account the coordinates from the individual GPS/EGNOS and GPS/SDCM solution as well as correction coefficients that are a function of the inverse of the ionospheric vertical TEC (VTEC) delay. Next the accuracy term was estimated in the form of the position errors and root mean square (RMS) errors. Finally the Kalman filter algorithm was used for improved the position errors and RMS errors. The developed algorithm is concerned with determining the positioning accuracy of the UAV for BLh (B-latitude, L-longitude, h-ellipsoidal height) ellipsoidal coordinates. The algorithm was tested on kinematic Global Positioning System/Satellite Based Augmentation System (GPS/SBAS) data recorded by a Global Navigation Satellite System (GNSS) receiver placed on a DJI Matrice 300RTK type unmanned platform. As part of the research test, two flights of the UAV were performed on 16 March 2022 in Olsztyn. In the first flight, the proposed algorithm enabled an increase in UAV positioning accuracy from 4% to 57% after Kalman filter process. In the second flight, on the other hand, UAV positioning accuracy was increased from 6% to 42%. The developed algorithm enabled an increase in UAV positioning accuracy and was successfully tested in two independent flight experiments. Ultimately, further research is planned to modify the algorithm with other correction coefficients.

Keywords: UAV, EGNOS, SDCM, accuracy, ionosphere delay.

INTRODUCTION

In recent years, there has been a noticeable increase in the number of unmanned aerial vehicle (UAV) platforms being operated and simultaneously used in various types of flight operations [1]. This has implications for improving the real-time positioning and navigation of UAVs [2],

which in turn affects the safety of flight execution [3]. In the aspect of UAV positioning in air navigation, Global Navigation Satellite System (GNSS) technology offers great opportunities [4]. In this sense, we can use it to determine the position, as well as other navigation parameters of the UAV flight such as speed or orientation in space [5]. For GNSS measurements, we can use

both absolute positioning methods and differential techniques [6]. The vast majority of GNSS receivers mounted on UAV platforms are single-frequency receivers designed for absolute positioning. It should be noted that this is mainly for L1 frequency code positioning in GNSS navigation systems. And in this case, the single point positioning (SPP) absolute positioning method is commonly used to determine the position of the UAV during flight [7]. However, the problem with this positioning method is the low accuracy of the determined user coordinates [8]. Therefore, it becomes necessary to develop algorithms to improve code-based positioning for UAV platforms. And here it should be noted that a very interesting position navigation solution in the SPP code method is the use of satellite based augmentation system (SBAS) corrections [9]. Such a solution allows improving GNSS positioning quality parameters, i.e. availability, continuity, accuracy and integrity [10]. Among the mentioned GNSS positioning quality parameters, this paper will present the results of UAV positioning accuracy with SBAS ionospheric correction. It is noteworthy that in recent years, increasingly rapid changes in the activity of the ionosphere have been noticed, which may affect the disruption of GNSS positioning [11], including UAV positioning.

STATE OF THE ART REVIEW OF THE RESEARCH TOPIC

The analysis of the state of the art is limited to presenting a literature review of the topic under discussion for European Geostationary Navigation Overlay Service (EGNOS) and System for Differential Corrections and Monitoring (SDCM) [12] as SBAS augmentation systems, whose correction coverage includes the area of Poland [13]. Therefore, the focus is on showing research papers that demonstrate the modelling of the ionospheric correction from an EGNOS or SDCM solution and its impact on the determination of the user's position. In the general scheme, each SBAS ionospheric model is defined by a regular grid with a spatial resolution of $5^\circ \times 5^\circ$ [14]. In each point of this grid, the ionospheric correction is expressed by the VTEC coefficient [15] or equivalently can be specified by the grid ionospheric vertical error (GIVE) parameter [16]. Numerous examples

of the use of EGNOS or SDCM augmentation systems for modelling the ionospheric correction or applying it to GNSS satellite positioning can be found in research papers. For example, the paper [17] shows the influence of the ionospheric perturbation from the EGNOS model on the determination of GNSS positioning quality parameters. The study shows that the higher the VTEC value, the worse the GNSS positioning quality parameters become. On the other hand, the paper [18] measured the values of VTEC and GIVE parameters from the EGNOS ionospheric model during the implementation of an airborne experiment. The next paper [19] presented a scheme for determining the ionospheric correction using the EGNOS augmentation system with reference to the GPS navigation system. In a subsequent paper [20], various research aspects concerning the modelling of the ionospheric disturbance with the EGNOS augmentation system were addressed. In another paper [21], the influence of selected ionospheric models, i.e. the Klobuchar model, the EGNOS model and the NeQuick model, on the accuracy of reference station coordinate determination during the occurrence of a geomagnetic storm in the ionosphere was presented. A similar study was performed in work [22], where the effect of ionospheric delay models from GPS, Galileo (European navigation satellite system), EGNOS and BeiDou (Chinese navigation satellite system) on the accuracy of UAV position determination during a test flight was shown. A very interesting study is shown in paper [23], where the authors presented a method for determining the integrity parameters horizontal protection level (HPL) and vertical protection level (VPL) with EGNOS ionospheric correction. For the aviation industry, important research was shown in paper [24], which presented the impact of EGNOS ionospheric correction on the availability of a position navigation solution within the SBAS approach with vertical guidance (APV) and localizer performance with vertical guidance 200 (LPV200) approach procedures. It is worth noting that in papers [25, 40, 41], the EGNOS ionospheric model was used as part of the development of an SBAS augmentation system for the Algerian area. In addition, publication [26] addressed the problem of extending the ionosphere model to the east of Poland. The paper compares VTEC values from the EGNOS ionosphere model and the Global ionosphere maps (GIM)

global ionosphere model from the international GNSS service (IGS). The research assumptions from the paper [26] were used in the paper [27], which showed the importance of the EGNOS ionosphere model for the SBAS APV approach procedure. The GIM global ionosphere model, on the other hand, proved to be effective in the non-precision approach (NPA) GNSS approach procedure. A study of the ionospheric correction in eastern Europe is shown in the work [28], which compares VTEC results from the EGNOS model and NeQuick 2. The difference in VTEC values does not exceed 1.5 TECU, which shows a good fit of both ionosphere models for the eastern European area and the possibility to adapt the VTEC parameter from another ionosphere model for the EGNOS augmentation system. The paper [29] showed the influence of selected ionospheric correction models, including from the EGNOS model, on the determination of aircraft position. It was found that the EGNOS ionospheric model gives similar results to the global GIM ionospheric model. A similar study was conducted in the article [30], which showed the results of aircraft positioning accuracy in the context of VTEC coefficient determination from the EGNOS ionosphere model. The article [31] shows how the ionospheric correction affects the monitoring and tracking of GNSS observations by EGNOS ranging integrity monitoring stations (RIMS) stations located in the northern part of Europe. In this context, a similar study was carried out in paper [32], which monitored scintillation changes in the ionosphere based on the EGNOS model for selected RIMS stations. An important study was also shown in paper [33], in which ionospheric delay values from the GPS, Galileo and EGNOS model were compared with respect to the GIM global ionosphere model from the IGS. It should be noted that the study shows the effect of ionospheric delay on the determination of DCB (differential code biases) instrumental errors. Publication [34] describes the concept of determining the ionospheric delay from the EGNOS model based on dual-frequency SBAS observations. This is an extremely interesting solution that will de facto apply to the future of EGNOS and the further operation of the space segment. On the other hand, the paper [35] presents the concept of using VTEC ionospheric delay in differential real time kinematic (RTK) measurements using RIMS stations. In aeronautical research, it is worth mentioning the

publications [13, 36], which show the results of monitoring changes in VTEC ionospheric delay during the execution of a test flight.

As the literature shows, far fewer scientific papers deal with the determination of the ionospheric correction from the SDCM model. It is noteworthy that the papers [13, 37] show the results of the ionospheric delay during the flight test. Subsequently, the work [38] presented ionospheric correction values from SDCM, EGNOS, GPS aided geo augmented navigation (GAGAN), wide area augmentation system (WAAS) and multi-functional satellite augmentation system (MSAS) for selected IGS reference stations. Similar comparative studies were also performed in paper [39], which showed ionospheric correction results from SDCM, EGNOS and GAGAN. In another publication [42], a method was developed to study the state of the ionosphere using Globalnaja nawigacionnaja sputnikowaja sistemiema (GLONASS) and SDCM signals. In turn, the paper [43] showed that the ionospheric correction from the SDCM model is better than from the WAAS model for the Russian Federation area. On the other hand, work [44] showed the possibility of using SDCM ionospheric correction for SBAS positioning in the area of South Korea.

The following conclusions are drawn from the state of the art analysis presented:

- the problem of modelling the ionospheric correction from an EGNOS and/or SDCM model is extremely important in the context of aeronautical applications,
- as the literature shows, research into the impact of the EGNOS and/or SDCM ionospheric correction on the determination of the position of a moving object is also extremely important in air transport,
- the obtained results of the VTEC ionospheric delay from the EGNOS and/or SDCM solution show a high convergence with the GIM global ionosphere model from the IGS, which allows their universal application in navigation and geodetic applications,
- the SBAS ionosphere model (EGNOS and/or SDCM) has been repeatedly used in the analysis and evaluation of the positioning accuracy of a moving object,
- determination of ionospheric delay from the EGNOS and/or SDCM model is crucial in the SBAS APV landing approach procedure.

RESEARCH PROBLEM

As the current state of knowledge in the research area shows, the use of SBAS ionospheric correction in aircraft or UAV positioning is becoming the basic standard these days when it comes to analysing the state of the ionosphere in GNSS measurements. Therefore, it is extremely important to study the impact of ionospheric correction on the user's positioning process itself and, at the same time, on positioning accuracy. From the literature, we can see that for GPS/SBAS positioning accuracy in air navigation, mainly a single GPS/EGNOS or GPS/SDCM solution has been used. From this point of view, it seems important to develop a mathematical combination for determining the positioning accuracy using EGNOS and SDCM data.

Accordingly, this article proposes the novelty as a the development of an algorithm for integrating the GPS/EGNOS + GPS/SDCM positioning model using modified weighting factors. In this sense, measurements weights were adopted as the inverse of the ionospheric delay determined separately from EGNOS and SDCM. And the GPS/EGNOS+GPS/SDCM positioning model itself was based on the weighted average model algorithm. Proposed algorithms have been developed to study the accuracy of BLh ellipsoidal coordinates determination for UAV technology. Moreover, the mentioned algorithms were tested in two UAV flight experiments. In addition, the Kalman filter was used in the accuracy analysis for the purpose of increasing the accuracy of GPS/EGNOS+GPS/SDCM positioning. As we have already mentioned, the methodology uses the weighted average model algorithm for the GPS/EGNOS+GPS/SDCM solution, which is based on a single GPS+EGNOS and GPS+SDCM solution. In turn, the coordinates of the position in a single GPS/EGNOS (or GPS/SDCM) solution are determined by the least squares method using the SPP code method. So, the determined coordinates may contain outlier measurements.

The use of the Kalman filter eliminates random errors and smooths the coordinates relative to the flight reference position in the time series. Therefore, the use of the Kalman filter should be understood in the context of improving the results relative to the least-squares solution.

RESEARCH METHODOLOGY

A schematic of the research methodology is shown in Figure 1. First, the GNSS satellite data, i.e. GPS observations and ephemeris data, and corrections from EGNOS and SDCM augmentation system, respectively, are recorded. Based on the collected GPS+SBAS data by the on-board GNSS receiver, the UAV position is determined using the SPP code method algorithm [13]. The determined UAV position in the form of BLh ellipsoidal coordinates is determined with an interval of 1 s for all recorded measurement epochs [8].

Such a scenario is implemented in a single GPS+SBAS kinematic solution [37], such as GPS+EGNOS or GPS+SDCM. However, having EGNOS and SDCM correction data, it is possible to develop an algorithm for integrating position determination based on the weighted average model [45], as shown in Figure 1. In this case, it is necessary to use appropriate measurement weights, which are also correction factors in the weighted average model in the joint GPS/EGNOS+GPS/SDCM position solution. So, the measurement weights used will have a decisive influence on the value of the determined UAV position coordinates in the GPS/EGNOS+GPS/SDCM solution. The paper proposes to use measurement weights as a function of SBAS ionospheric delay. Then the basic observation equation in the weighted average model in the joint GPS/EGNOS+GPS/SDCM position solution will take the form:

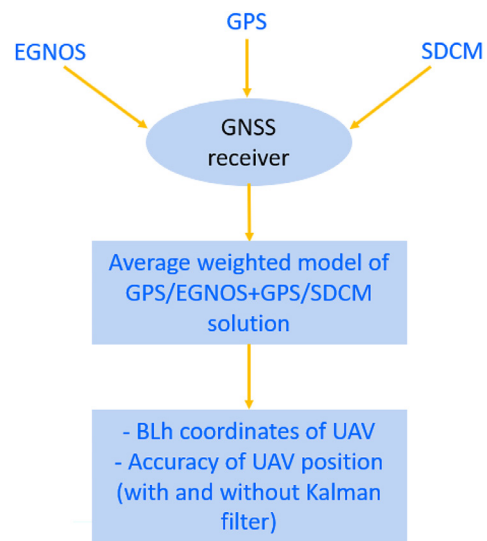


Figure 1. The flowchart of presented research methodology

$$\begin{cases} B_m = \frac{A1 \cdot B_{G/E} + A2 \cdot B_{G/S}}{A1 + A2} \\ L_m = \frac{A1 \cdot L_{G/E} + A2 \cdot L_{G/S}}{A1 + A2} \\ h_m = \frac{A1 \cdot h_{G/E} + A2 \cdot h_{G/S}}{A1 + A2} \end{cases} \quad (1)$$

where: (B_m, L_m, h_m) – final position of the UAV, $(A1, A2)$ – correction coefficients, $A = \frac{1}{ION_E}$ – correction coefficient for EGNOS, $B = \frac{1}{ION_S}$ – correction coefficient for SDCM, ION_E – ionospheric delay value from the EGNOS model, ION_S – ionospheric delay value from the SDCM model, $(B_{G/E}, L_{G/E}, h_{G/E})$ – UAV position from the GPS/EGNOS solution, $(B_{G/S}, L_{G/S}, h_{G/S})$ – UAV position from the GPS/SDCM solution.

The SBAS ionospheric delay parameters (ION_E, ION_S) will be expressed by the VTEC coefficient, which determines the electron content of the ionosphere along the path of the satellite signal from the satellite to the GNSS receiver [46]. The value of the VTEC coefficient is separately determined from EGNOS and SDCM system. Then the measurement weights (A1, A2) will be respectively:

$$\begin{cases} A1 = \frac{1}{ION_E} = \frac{1}{VTEC_E} \\ A2 = \frac{1}{ION_S} = \frac{1}{VTEC_S} \end{cases} \quad (2)$$

And in turn, Equation 1 will then take the form:

$$\begin{cases} B_m = \frac{\frac{1}{VTEC_E} \cdot B_{G/E} + \frac{1}{VTEC_S} \cdot B_{G/S}}{\frac{1}{VTEC_{EGNOS}} + \frac{1}{VTEC_{SDCM}}} \\ L_m = \frac{\frac{1}{VTEC_E} \cdot L_{G/E} + \frac{1}{VTEC_S} \cdot L_{G/S}}{\frac{1}{VTEC_{EGNOS}} + \frac{1}{VTEC_{SDCM}}} \\ h_m = \frac{\frac{1}{VTEC_E} \cdot h_{G/E} + \frac{1}{VTEC_S} \cdot h_{G/S}}{\frac{1}{VTEC_E} + \frac{1}{VTEC_S}} \end{cases} \quad (3)$$

Equation 3 is the basic mathematical model for determining UAV position according to the submitted test method. Next, the UAV positioning accuracy is determined in the flowchart in the form of position errors and RMS mean-square errors for all BLh components. The position errors are determined according to the relationship:

$$\begin{cases} \Delta B = B_m - B_r \\ \Delta L = L_m - L_r \\ \Delta h = h_m - h_r \end{cases} \quad (4)$$

where: $(\Delta B, \Delta L, \Delta h)$ – positioning accuracy of the UAV [37, 47], (B_r, L_r, h_r) – UAV reference coordinates from the PPK (post processing kinematic) solution.

In turn, RMS errors were calculated according to the relationship:

$$\begin{cases} RMS\Delta B = \sqrt{\frac{[\Delta B^2]}{N}} \\ RMS\Delta L = \sqrt{\frac{[\Delta L^2]}{N}} \\ RMS\Delta h = \sqrt{\frac{[\Delta h^2]}{N}} \end{cases} \quad (5)$$

where: $RMS\Delta B, RMS\Delta L, RMS\Delta h$ – RMS error for each axes of BLh coordinates, N – total number of observations.

Equations 4–5 are computational algorithms for determining UAV positioning accuracy from a joint GPS/EGNOS+GPS/SDCM solution. Moreover, the parameters $(\Delta B, \Delta L, \Delta h)$ will be determined for each measurement epoch during the UAV flight. In turn, the parameters $RMS\Delta B, RMS\Delta L, RMS\Delta h$ will be determined as a single resultant value of position error for all recorded measurement epochs. At this stage, it is possible to use the Kalman filter for the purpose of increasing the accuracy of UAV positioning from a joint GPS/EGNOS+GPS/SDCM solution. The Kalman filter is a two-stage mathematical algorithm consisting of a prediction stage (time update) and a correction stage (measurement update). The equations in the prediction stage can be written as follows [48]:

$$\begin{cases} \bar{x}(k) = G \cdot x(k-1) \\ \bar{P}(k) = G \cdot P(k-1) \cdot G^T + Q(k) \end{cases} \quad (6)$$

where: G – coefficient matrix, $x(k-1)$ – estimated values of the determined a priori parameters from the previous step, $P(k-1)$ – estimated values of the a priori covariance matrix from the previous step, $\bar{x}(k)$ – state value forecast, $\bar{P}(k)$ – predicted values of the covariance matrix, $Q(k)$ – covariance matrix of the noise process, $(k-1)$ – previous measurement epoch, k – current measurement epoch.

In turn, the mathematical equations in the correction stage can be written as follows [49]:

$$\begin{cases} K(k) = \bar{P}(k) \cdot H^T \cdot (H \cdot \bar{P}(k) \cdot H^T + PR)^{-1} \\ x(k) = \bar{x}(k) + K(k) \cdot (z - H \cdot \bar{x}(k)) \\ P(k) = (I - K(k) \cdot H) \cdot \bar{P}(k) \end{cases} \quad (7)$$

where: PR – measurement covariance matrix, H – partial derivative matrix, $K(k)$ – Kalman gain matrix, z – vector of measured quantities, I – unit matrix, $x(k)$ – a posteriori state

vector estimate, $P(k)$ – a posteriori covariance matrix of the determined parameters.

For the purpose of the implemented calculations in the case under study, the following boundary values were assumed in the Kalman filtration process [48]:

- parameter $G = \begin{bmatrix} 1 & 0 & 0 \\ 0 & 1 & 0 \\ 0 & 0 & 1 \end{bmatrix}$,
- parameter $P(k-1) = \begin{bmatrix} 10^1 & 0 & 0 \\ 0 & 10^1 & 0 \\ 0 & 0 & 10^1 \end{bmatrix} \text{ m}^2$,
- parameter $Q(k) = \begin{bmatrix} 10^{-2} & 0 & 0 \\ 0 & 10^{-2} & 0 \\ 0 & 0 & 10^{-2} \end{bmatrix} \text{ m}^2$,
- based on matrix $Q(k)$ the process noise values are $W_k = 0.1 \text{ m}$ along the individual BLh coordinate axes,
- parameter $H = \begin{bmatrix} 1 & 0 & 0 \\ 0 & 1 & 0 \\ 0 & 0 & 1 \end{bmatrix}$,
- parameter $PR = \begin{bmatrix} 3 & 0 & 0 \\ 0 & 3 & 0 \\ 0 & 0 & 3 \end{bmatrix} \text{ m}^2$,
- based on matrix PR the noise values of the observation model are $V_k = 1.75 \text{ m}$ for the individual BLh position components, in this case the distribution of measurement errors has white noise,
- parameter $z = \begin{bmatrix} \Delta B \\ \Delta L \\ \Delta h \end{bmatrix} \text{ m}$.

In this work, we applied the standard Kalman filter for the linear system model. We were only concerned with improving the determination of positions and their accuracy, which is crucial under ICAO’s SBAS recommendation and certification. Had we additionally determined the velocity then the extended Kalman filter (EKF) can be applied.

According to the flowchart in Figure 1, the presented calculation procedure is performed in parallel for all 3 BLh components under GPS/EGNOS+GPS/SDCM positioning. The input data for accuracy calculations are the user expressed coordinates and the flight reference coordinates. Position errors and RMS errors are then determined based on Equations 4–7. This will give the final GPS/EGNOS+GPS/SDCM positioning accuracy with and without the use of Kalman filtering. Based on this, it will be possible to further compare the obtained GPS/SBAS positioning accuracy results. The mathematical model specified in this way is intended to improve the final UAV positioning

accuracy based on measurement data from the two SBAS support systems. The functioning of the algorithm was tested in two independent UAV flight experiments.

RESEARCH TEST

The main objective of the research test was to verify the developed mathematical algorithm in practice. On this basis, two independent flights were performed using a DJI Matrice 300RTK UAV platform. The Matrice 300 RTK is the latest industrial drone developed by DJI Enterprise. The drone has a flight range of up to 8 kilometers and a flight time of up to 55 minutes. It has sensors that operate in 6 directions. The DJI Matrice 300 RTK allows you to customize the equipment for your individual task. Up to 3 devices can be mounted on the drone simultaneously, with a total maximum weight of up to 2.7 kg. The DJI Matrice 300 RTK has a set of sensors, safety and redundancy systems that inform about flight, navigation or obstacles. We are talking about such sensors as two gyroscopes, barometers, RTK GNSS antennas and compasses, six pairs of optical sensors [50].

The flight experiments were performed on 16 March 2022. The first flight test lasted from 11:00:26 (39626 s) to 11:15:18 (40518 s) according to GPS Time. Figures 2 and 3 show the horizontal trajectory of the UAV flight and the change in flight altitude as a function of time in Experiment 1, respectively.

The second flight test lasted from 14:28:54 (52134 s) to 14:44:17 (53057 s) according to GPS Time. Figures 4 and 5 show the horizontal trajectory of the UAV flight and the change in flight altitude as a function of time in Experiment 2, respectively. In Figures 3, 5, 6–15, the UAV’s flight turns are marked as red dots.

The GNSS receiver placed on the UAV platform recorded GPS and SBAS satellite data, which were used to determine the position from the EGNOS and SDCM solution. The UAV position coordinates were calculated using RT-KLIB v.2.4.3 [51]. In addition, the UAV flight reference trajectory, for the purpose of calculating positioning accuracy from a single EGNOS and SDCM solution, was determined in Topcon MAGNET Tools v.5.1.1.0 [52]. Finally, the developed algorithm (1–7) was implemented in the Scilab v.6.1.1 language [53], in which an author’s script was written to implement the

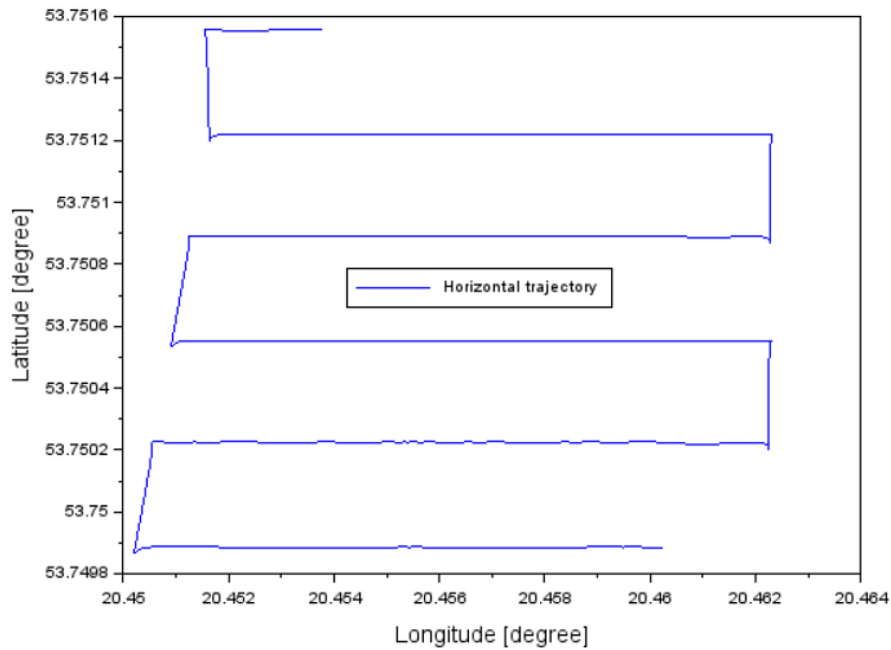


Figure 2. Horizontal trajectory of the UAV during flight 1

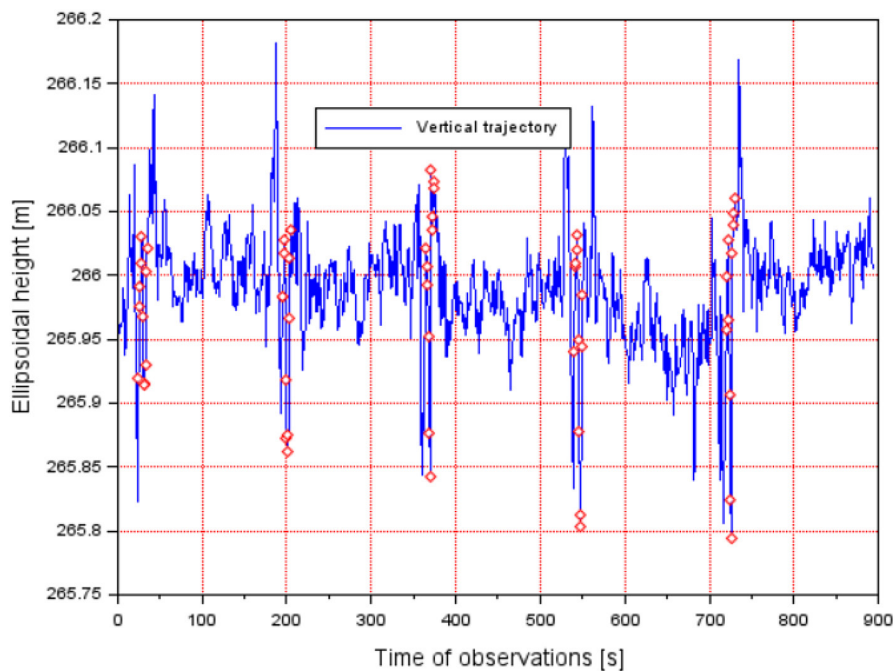


Figure 3. Change in flight altitude of the UAV during flight 1

calculation of the EGNOS+SDCM positioning accuracy. The results were obtained from the proposed EGNOS+SDCM solution.

RESEARCH RESULTS AND DISCUSSION

The description of the obtained research results started with the presentation of the observational

conditions during the implemented experiments, i.e. determination of the number of tracked satellites, determination of the PDOP (Position DOP) value, determination of the state of the ionosphere. Figures 6 and 7 show the number of tracked GPS satellites for which corrections from EGNOS and SDCM were determined. In Experiment 1, the number of GPS satellites with EGNOS corrections available was between 9 and 10. In contrast, the

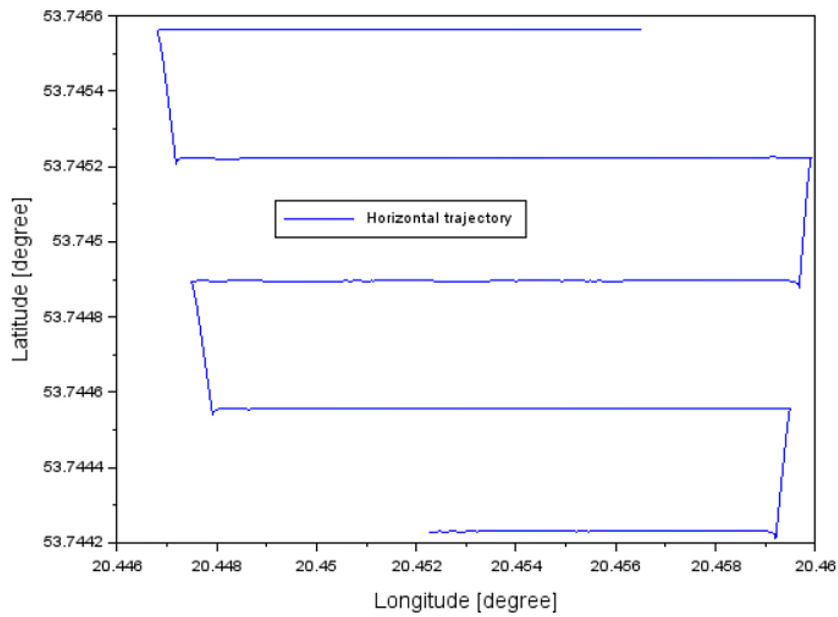


Figure 4. Horizontal trajectory of the UAV during flight 2

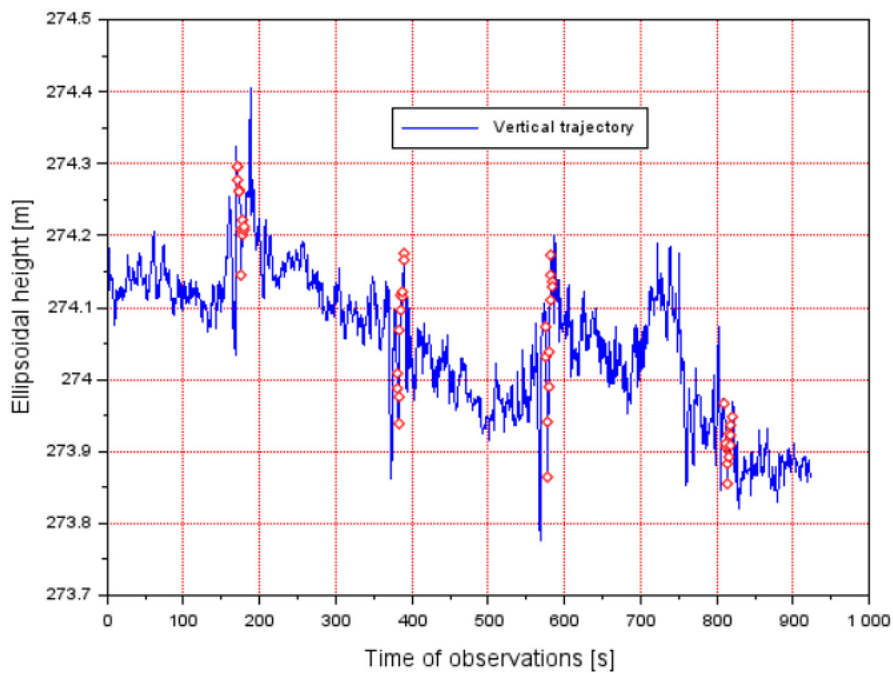


Figure 5. Change in flight altitude of the UAV during flight 2

number of GPS satellites with SDCM corrections available was between 6 and 8, respectively. It can be seen that EGNOS gave corrections for more GPS satellites than the SDCM augmentation system.

In Experiment 2, the number of GPS satellites with available EGNOS corrections was between 7 and 10, while the number of GPS satellites with available SDCM corrections was also between 7 and 10.

Following this, Figures 8 and 9 show the PDOP values [54] during flight 1 and 2. Thus, during flight 1, the PDOP values are respectively: 2.04 to 2.25 for the GPS/EGNOS solution and 1.66 to 2.31 for the GPS/SDCM solution.

During flight 2, the PDOP values were: between 2.21 and 2.68 for the GPS/EGNOS solution and between 1.53 and 1.93 for the GPS/SDCM solution. As can be observed, the PDOP

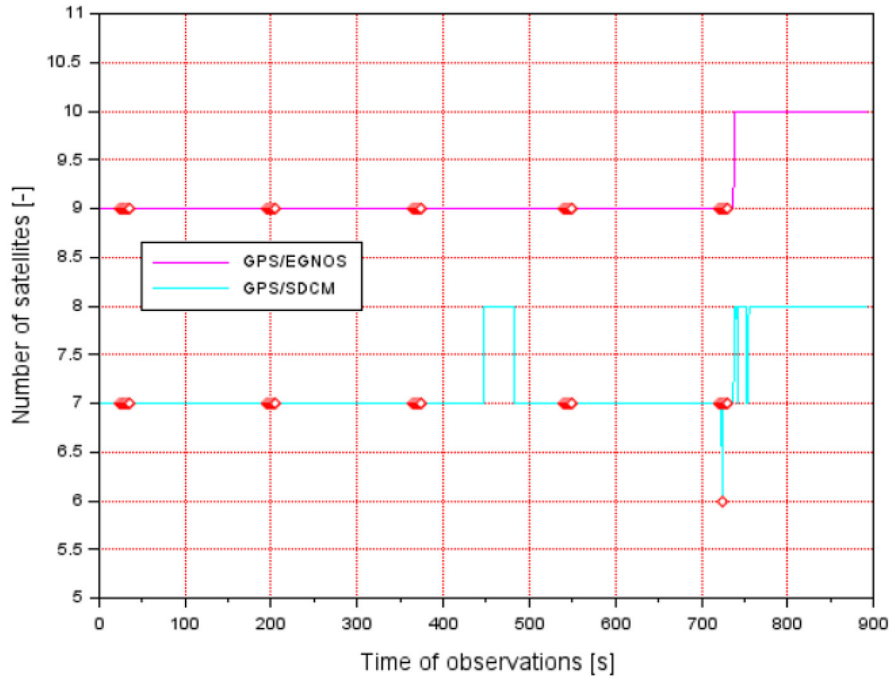


Figure 6. Number of GPS satellites tracked with SBAS corrections during flight 1

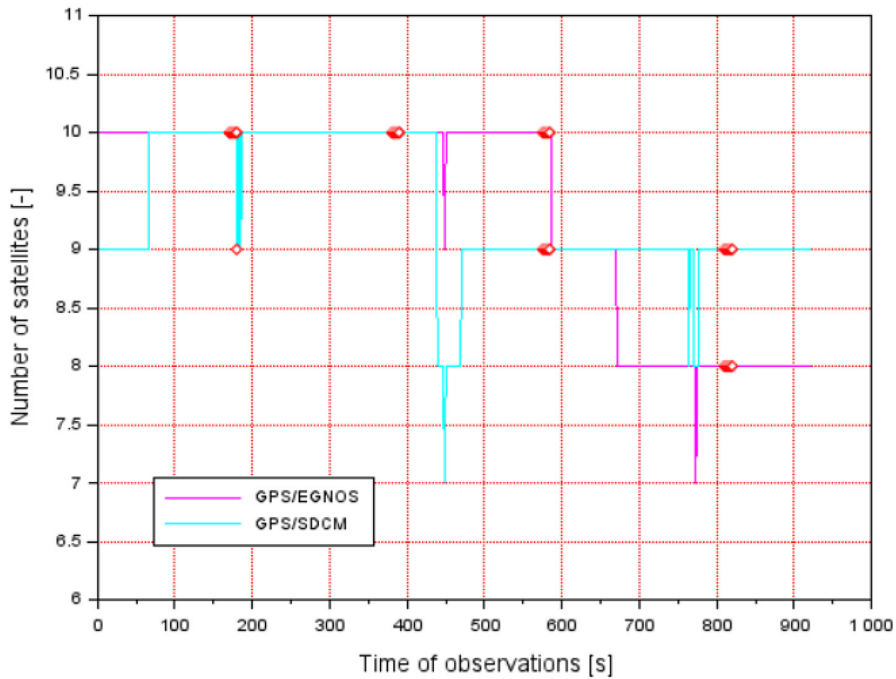


Figure 7. Number of GPS satellites tracked with SBAS corrections during flight 2

values were lower for the GPS/SDCM solution than for GPS/EGNOS.

Subsequently, Table 1 shows the values of the ionospheric state during flight 1 and flight 2. For this purpose, the values of the ionospheric VTEC delay were determined from the grid of the EGNOS and SDCM model. In the case

of the EGNOS model, the value of the VTEC parameter varies from 3.125 m to 3.250 m in flight 1 and from 2.750 m to 2.875 m in flight 2. In the SDCM, on the other hand, the value of the ionospheric VTEC correction is constant at 3.375 m in flight 1 and 2.500 m in flight 2. As shown in Table 1, a higher value of ionospheric

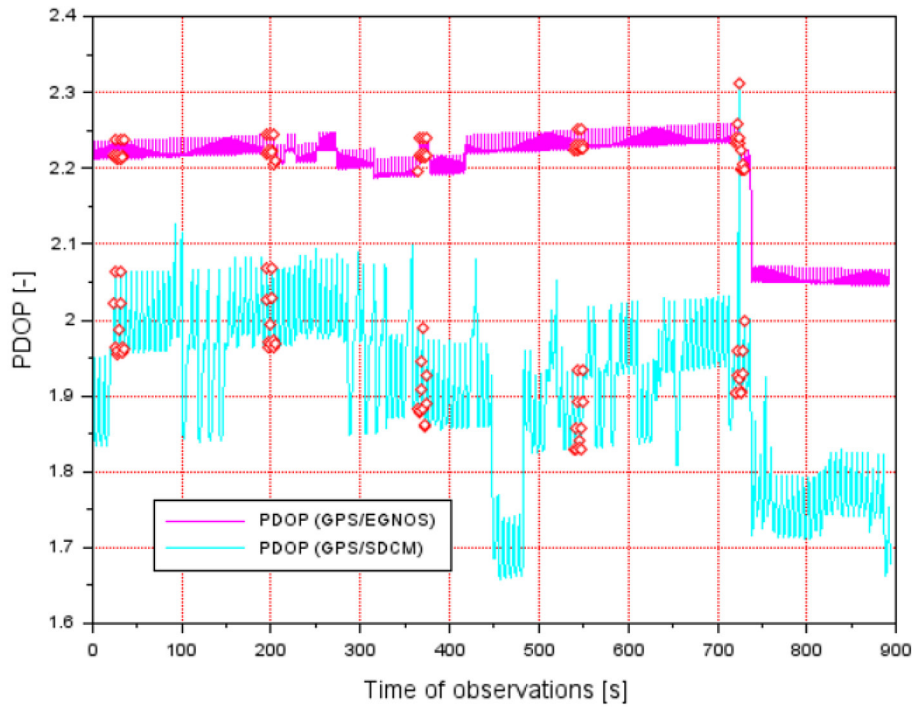


Figure 8. PDOP values during flight 1

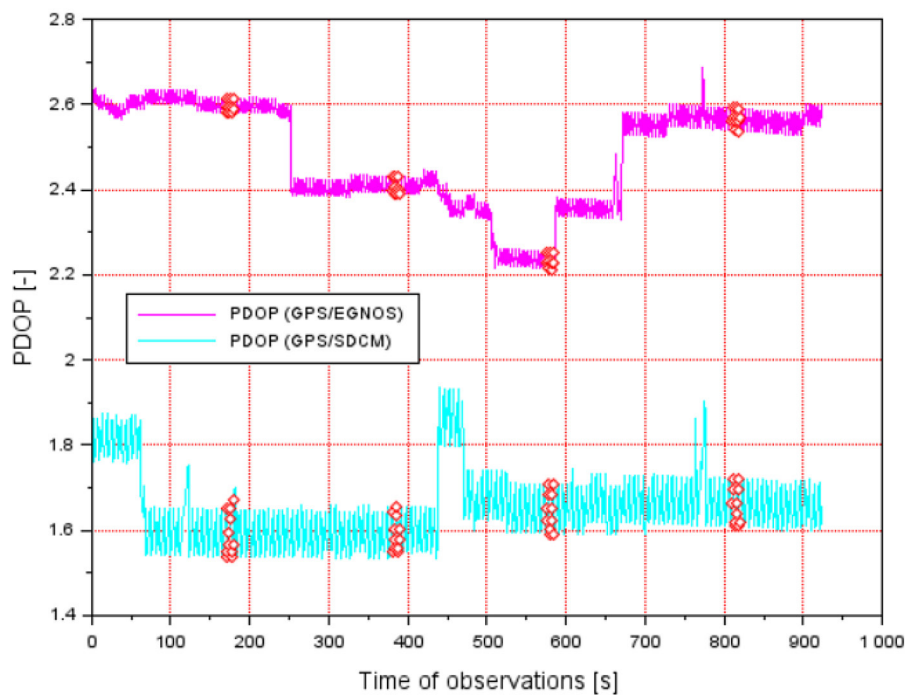


Figure 9. PDOP values during flight 2

disturbance is seen in the EGNOS model than in the SDCM model.

The computed values of the VTEC parameter allowed the determination of the correction coefficients (A_1 , A_2) from the mathematical model (1–3). Hence, the results of the correction coefficients (A_1 , A_2) are shown in Table 2. In the case

of the EGNOS model, the value of the A_1 coefficient varies from 0.308 to 0.320 in flight 1 and from 0.348 to 0.363 in flight 2. In the SDCM, on the other hand, the value of the A_2 coefficient is constant at 0.296 in flight 1 and 0.400 in flight 2.

By determining the values of the correction coefficients (A_1 , A_2) from the mathematical

Table 1. Comparison of VTEC values for the EGNOS and SDCM solution during flight 1 and 2

Flight experiment	VTEC value based on EGNOS model [m]	VTEC value based on SDCM model [m]
Flight 1	From 3.125 to 3.250	3.375
Flight 2	From 2.750 to 2.875	2.500

Table 2. Comparison of correction coefficients (A1, A2) during flight 1 and 2

Flight experiment	Correction coefficient A1 value based on the EGNOS model [-]	Correction coefficient A2 value based on the SDCM model [-]
Flight 1	From 0.308 to 0.320	0.296
Flight 2	From 0.348 to 0.363	0.400

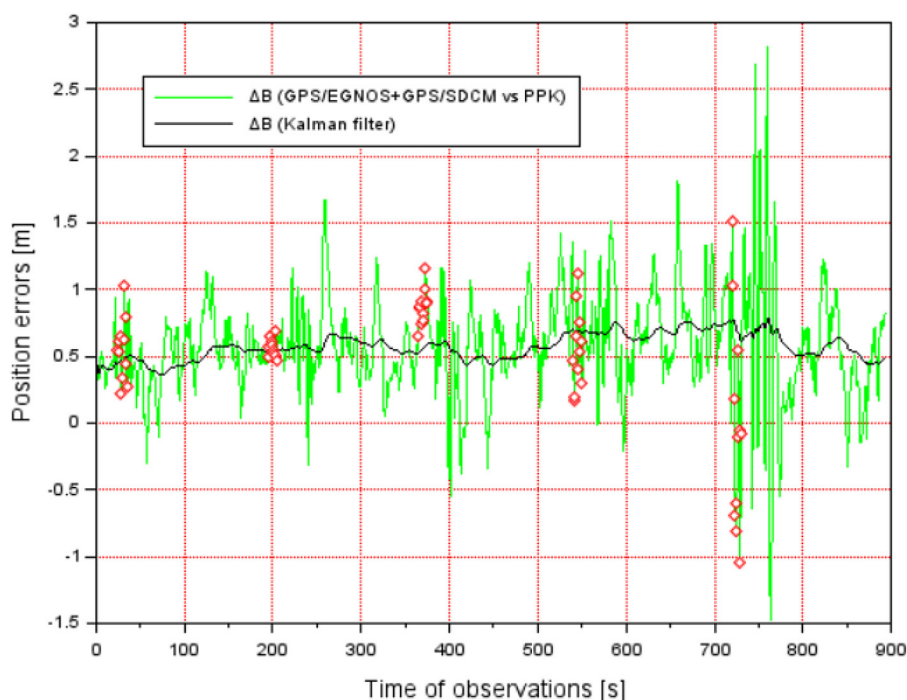


Figure 10. Position error values for the B component during flight 1

model (1–3), it was possible to determine the resultant positioning accuracy of EGNOS+SDCM using the proposed mathematical model (4–7). Therefore, the results of the UAV positioning accuracy are presented in Figures 10–15. First, Figures 10 and 11 show the position error results for the B component from flight 1 and flight 2. During flight 1, the position errors for the B component were -1.48 m to +2.82 m for the GPS/EGNOS+GPS/SDCM solution, and +0.36 m to +0.80 m for the Kalman filter method, respectively. Furthermore, the RMS errors [55] were respectively: 0.70 m for the GPS/EGNOS+GPS/SDCM solution, and 0.58 m for the Kalman filter algorithm.

On the other hand, during flight 2, the position errors for the B component were -2.14 m

to +1.89 m for the GPS/EGNOS+GPS/SDCM solution, and -0.05 m to +0.81 m for the Kalman filter model, respectively. In addition, the RMS errors were respectively: 0.64 m for the GPS/EGNOS+GPS/SDCM solution, and 0.55 m for the Kalman filter model. The outlier results of the position errors in Figure 10-11 are caused by the UAV’s change in direction, as shown by the red dots. Secondly, Figures 12 and 13 show the results of the position errors for the L component from flight 1 and flight 2. During flight 1, the position errors for the L component were -0.32 m to +1.81 m for GPS/EGNOS+GPS/SDCM solution, and +0.64 m to +0.96 m for the Kalman filter model, respectively. In addition, the RMS errors were respectively: 0.80 m for the GPS/



Figure 11. Position error values for the B component during flight 2

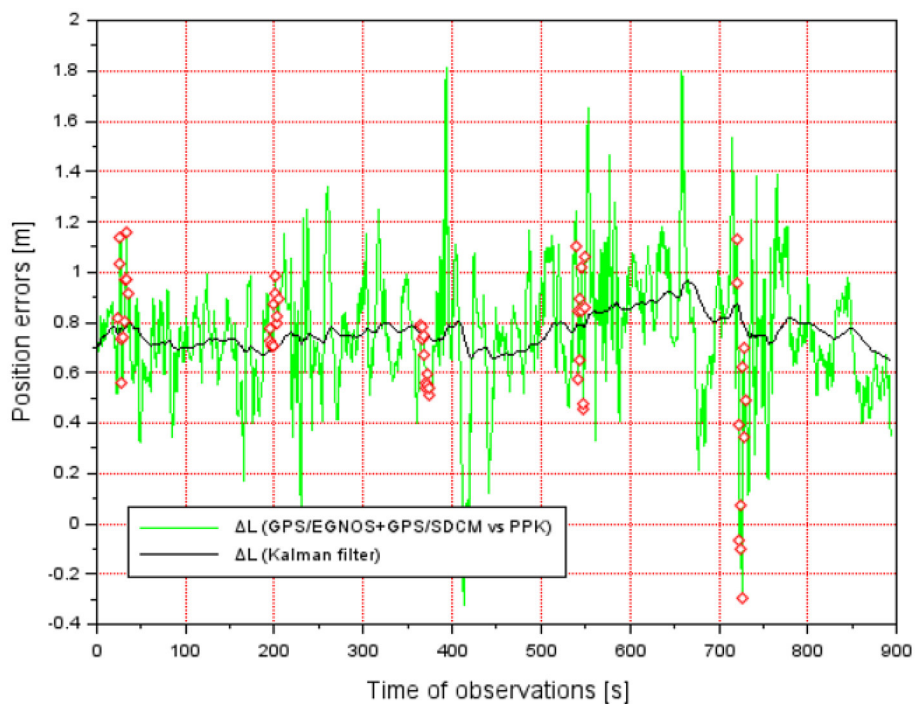


Figure 12. Position error values for the L component during flight 1

EGNOS+GPS/SDCM solution, and 0.76 m for the Kalman filter method.

On the other hand, during flight 2, the position errors for the L component were -1.33 m to +1.59 m for the GPS/EGNOS+GPS/SDCM solution, and +0.34 m to +1.33 m for the Kalman filter model,

respectively. In addition, the RMS errors were respectively: 0.75 m for the GPS/EGNOS+GPS/SDCM solution, and 0.70 m for the Kalman filter model. The outlier results of the position errors in Figure 12-13 are caused by the UAV's change in direction, as shown by the red dots.

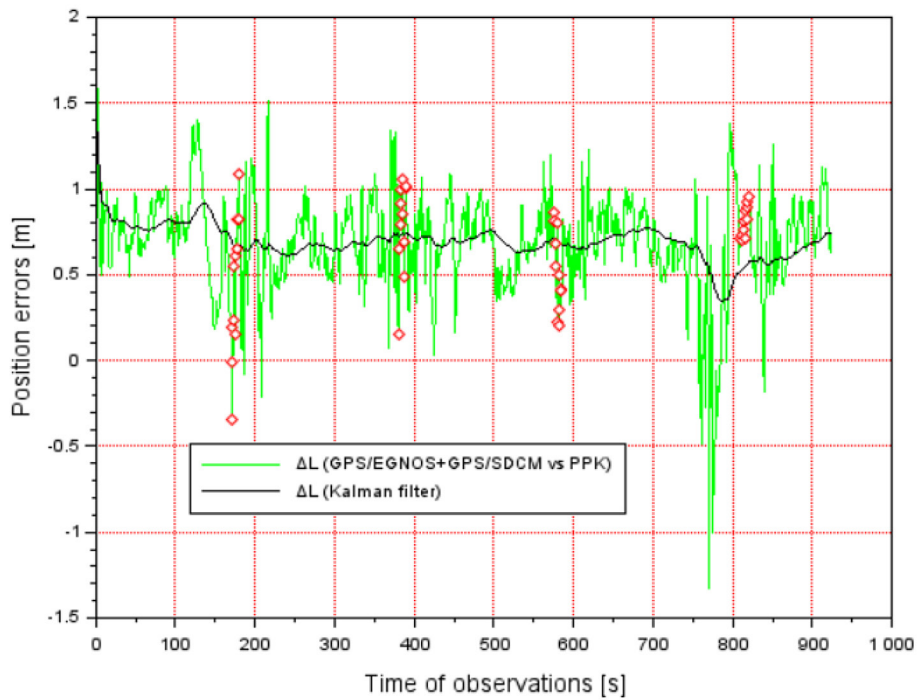


Figure 13. Position error values for the L component during flight 2

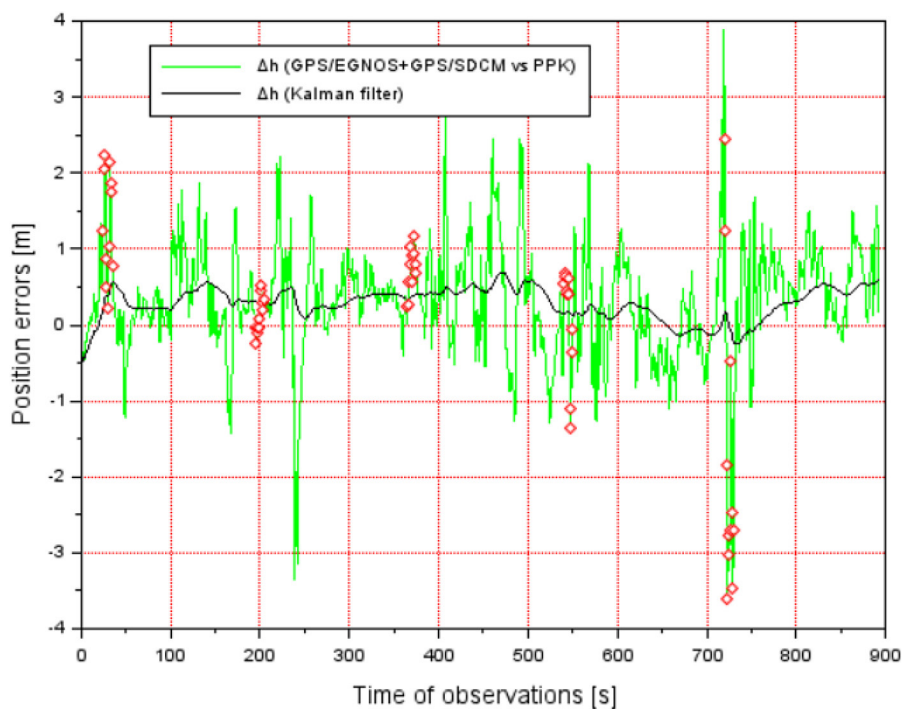


Figure 14. Position error values for the h component during flight 1

Finally, Figures 14 and 15 show the results of the position errors for the h component from flight 1 and flight 2. During flight 1, the position errors for the h component were -3.61 m to +3.90 m for the GPS/EGNOS+GPS/SDCM solution, and -0.52 m to +0.69 m for the Kalman filter model,

respectively. In addition, the RMS errors were respectively: 0.82 m for the GPS/EGNOS+GPS/SDCM solution, and 0.35 m for the Kalman filter model. In contrast, during flight 2, the position errors for the h component were -2.05 m to +3.17 m for the GPS/EGNOS+GPS/SDCM solution, and

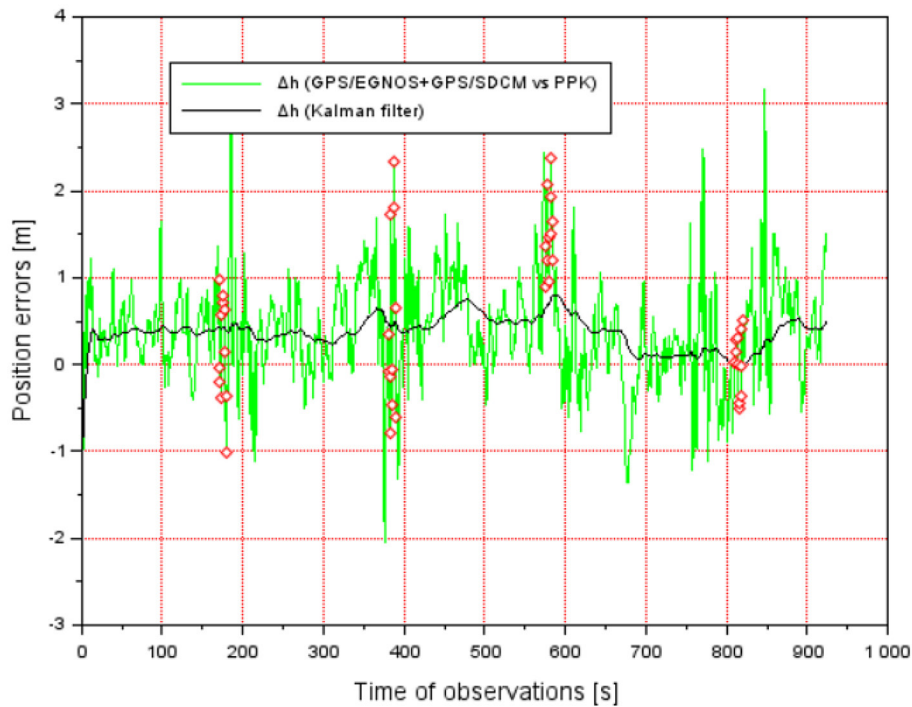


Figure 15. Position error values for the h component during flight 2

-0.84 m to +0.80 m for the Kalman filter model, respectively. In addition, the RMS errors were respectively: 0.71 m for the GPS/EGNOS+GPS/SDCM solution, and 0.41 m for the Kalman filter model. The outlier results of the position errors in Figure 14–15 are caused by the UAV’s change in direction, as shown by the red dots.

As part of the discussion to the research achieved, it was shown how the proposed solution from mathematical Equations 1–7 improved the positioning accuracy of the UAV. For this purpose, a comparison of the percentage of the obtained RMS errors for the GPS/EGNOS+GPS/SDCM, and Kalman filter model solution was made. When the Kalman filter algorithm is used in Experiment 1, the RMS errors improve: from 4% to 57% relative to the RMS errors determined for the GPS/EGNOS+GPS/SDCM solution. In contrast, in Experiment 2, the RMS errors for the Kalman filter algorithm are reduced: from 6% to 42% relative to the RMS errors determined for the GPS/EGNOS+GPS/SDCM solution. In addition, it is worth noting that the proposed mathematical algorithm (1–7) makes it possible to improve RMS accuracy by, respectively:

- 3% to 63% relative to a single GPS/EGNOS solution for flight 1,
- from 4% to 61% relative to a single GPS/SDCM solution for flight 1,

- 3% to 42% relative to a single GPS/EGNOS solution for flight 2,
- 10% to 44% relative to a single GPS/SDCM solution for flight 2.

Based on the comparison, it can be seen the high effectiveness of the proposed algorithm for improving UAV positioning accuracy. Thus, the adoption of the correction coefficient solution as a function of the inverse of the VTEC ionospheric correction proved to be correct and was verified positively. Moreover, the repeatability of the test method for different GNSS measurement data was maintained.

The second part of the discussion concerns the comparison of the obtained research results in the context of the literature. By comparing the obtained accuracy results for the applied research method in relation to the state-of-the-art analysis, it can be concluded that:

- the developed algorithm is part of the current research on improving positioning accuracy using GPS/EGNOS+GPS/SDCM solution in air transport similarly to the work [13],
- the paper shows the effect of SBAS ionospheric correction on the accuracy of position determination similarly to the works [21, 22, 29, 30],
- the developed algorithm allows for position error reduction, which has also been used in other works [48, 49],

- the results obtained highlight that the positioning accuracy using the GPS/EGNOS+GPS/SDCM solution is better than that using the GPS/EGNOS solution only, which has already been demonstrated in works [13].

CONCLUSIONS

This paper shows the results of a study to determine the positioning accuracy of GPS/EGNOS+GPS/SDCM for UAV technology. For this purpose, a mathematical model of average weighted was developed for determining the UAV position derived from the GPS/EGNOS+GPS/SDCM solution. In addition, the algorithm considers the correction coefficients that are a function of the inverse of the ionospheric VTEC delay from EGNOS and SDCM model. For the determined UAV coordinates from the weighted average model, their accuracy was determined in the form of position errors and RMS errors. Moreover, the Kalman filtering algorithms was used in accuracy analysis for position errors and RMS errors improved. The developed algorithm concerns the determination of UAV positioning accuracy for BLh ellipsoidal coordinates. The algorithm was tested on kinematic GPS/SBAS data recorded by a GNSS receiver placed on a DJI Matrice 300RTK UAV platform. As part of the research test, two UAV flights were performed on 16 March 2022 in Olsztyn. The tests were carried out at a time interval and took into account the change in the state of the ionosphere during the measurement. Numerical calculations were carried out using RTKLIB, Topcon MAGNET Tools and Scilab programmes. In the near future, the authors of the paper plan to continue research on modifying the algorithm with other correction coefficients. Moreover, the presented method can be a particularly useful in application of photogrammetry.

REFERENCES

1. Kustra M. Unmanned aerial systems - mobile monitoring in the state security system. In: *Modern Navigation*, vol. II, Dęblin, 2020, 305–313. (in Polish)
2. Wyszycacz W. The risk of threats management in the use of unmanned aerial vehicles, PhD Thesis, Poznan University of Technology, 2020, 1–151. (in Polish)
3. Fellner A. Precise pre-positioning and direct navigation preparation in RPAS operational work, In:

Unmanned aircraft systems in firefighting and rescue - from product to rescuer, Jozefów, 2022, 65–85.

4. Zawistowski M., Fellner R. Important parameters and settings in unmanned aerial vehicles (UAV) in operational work of the fire brigade. *Safety & Fire Technology*. 2021, 58(2), 92–118, <https://doi.org/10.12845/sft.58.2.2021.6>
5. Lalak M., Wierzbicki D., Kędzierski M. Methodology of processing single-strip blocks of imagery with reduction and optimization number of ground control points in UAV photogrammetry. *Remote Sens*. 2020, 12, 3336. <https://doi.org/10.3390/rs12203336>
6. Oleniacz G., Cwiąkała P., Gabryszuk J., et al. GNSS technology and its application in setting out surveys and monitoring. *Higher School of Engineering and Economics*, Rzeszów, 2015, 1–136.
7. Forlani G., Diotri F., Morra di Cella U., Roncella R. Uav block georeferencing and control by on-board gnss data. *ISPRS - International Archives of the Photogrammetry, Remote Sensing and Spatial Information Sciences*, 2020, 43B2, 9–16, <https://doi.org/10.5194/isprs-archives-XLIII-B2-2020-9-2020>
8. Wierzbicki D. The prediction of position and orientation parameters of UAV for video imaging. *The International Archives of the Photogrammetry, Remote Sensing and Spatial Information Sciences*. 2017, XLII-2(W6). <https://doi.org/10.5194/isprs-archives-XLII-2-W6-407-2017>
9. Grzegorzewski M. Navigating an aircraft by means of a position potential in three dimensional space, *Annual of Navigation*, 2005, 9, 1–111.
10. Kaleta W. EGNOS based APV procedures development possibilities in the south-eastern part Of Poland. *Annual of Navigation*, 2014, 21, 85–94.
11. GISPLAY website. Avialable from: <https://gisplay.pl/geo/10446-gugik-ostreza-przed-wplywem-jonosfery-na-dokladnosc-pomiarow-gnss.html>, (Accessed: 01.08.2023).
12. IGS webiste. Avialable from: <https://igs.org/mgex/constellations/#sbas>, (Accessed: 01.08.2023).
13. Mrozik M. Application of the SBAS positioning method in the aircraft approach procedure, PhD thesis. Silesian University of Technology, Gliwice, 2023, 1–147. (in Polish)
14. EGNOS fact sheet. Avialable from: http://www.egnos-pro.esa.int/Publications/2005%20Updated%20Fact%20Sheets/fact_sheet_2.pdf, (Accessed: 01.08.2023).
15. EGNOS OS Service definition Document. Avialable from: https://www.euspa.europa.eu/sites/default/files/brochure_os_2017_v6.pdf, (Accessed: 01.08.2023).
16. Jan S.-S., Chan W., Walter T. MATLAB algorithm availability simulation tool. GPS

- Solutions. 2009, 13(4), 327–332, <https://doi.org/10.1007/s10291-009-0117-4>
17. Ciećko A. Analysis of the EGNOS quality parameters during high ionosphere activity. *IET Radar Sonar Navigation*. 2019, 13, 1131–1139, <https://doi.org/10.1049/iet-rsn.2018.5571>
 18. Krasuski K., Jafernik H. Designation the EGNOS ionospheric corrections in flight test in Dęblin (01.06.2010). *Autobusy: technika, eksploatacja, systemy transportowe*. 2017, 18(6), 822–825. (in Polish)
 19. Arbesser-Rastburg B. Ionospheric Corrections for Satellite Navigation Using EGNOS, In *Proceedings of XXVII URSI General Assembly Conference, 2002, Maastricht (Netherlands)*, 1–306, <https://www.ursi.org/proceedings/procGA02/ursiga02.pdf>, (Accessed: 01.08.2023).
 20. Jakowski N., Leitinger R., Ciraolo L. Behaviour of large scale structures of the electron content as a key parameter for range errors in GNSS applications. *Annals of Geophysics*. 2004, Supplement to 47(2/3), 1031–1047, <https://doi.org/10.4401/ag-3284>
 21. Ciećko A., Grunwald G. Klobuchar, NeQuick G, and EGNOS Ionospheric Models for GPS/EGNOS Single-Frequency Positioning under 6–12 September 2017 Space Weather Events. *Applied Sciences*. 2020, 10, 1553, <https://doi.org/10.3390/app10051553>
 22. Grunwald G., Ciećko A., Kozakiewicz T., Krasuski K. Analysis of GPS/EGNOS positioning quality using different ionospheric models in UAV navigation. *Sensors*. 2023, 23, 1112, <https://doi.org/10.3390/s23031112>
 23. Lupsic B., Takács B. Analysis of the EGNOS ionospheric model and its impact on the integrity level in the Central Eastern Europe region. *Int. Arch. Photogramm. Remote Sens. Spatial Inf. Sci.* 2019, XLII-4/W14, 159–165, <https://doi.org/10.5194/isprs-archives-XLII-4-W14-159-2019>
 24. Trilles S., Authié T., Renazé C., Raoul O. Robust EGNOS Availability Performances under Severe Ionospheric Conditions. In: *Proceedings of the 28th International Technical Meeting of the Satellite Division of The Institute of Navigation (ION GNSS+ 2015)*, Tampa, Florida, September 2015, 1783–1789.
 25. Takka E., Belhadj-Aissa A., Yan J., Jin B., Bouaraba A. Ionosphere modeling in the context of Algerian Satellite-based Augmentation System. *Journal of Atmospheric and Solar-Terrestrial Physics*. 2019, Volume 193, 105092, <https://doi.org/10.1016/j.jastp.2019.105092>
 26. Świątek A., Stanisławska I., Zbyszyński Z., Dziak-Jankowska B. Extension of EGNOS ionospheric correction coverage area. *Acta Geophysica*. 2014, 62, 259–269, <https://doi.org/10.2478/s11600-013-0166-5>
 27. Grunwald G., Bakula M., Ciećko A. Study of EGNOS accuracy and integrity in eastern Poland. *The Aeronautical Journal*. 2016, 120(1230), 1275–1290, <https://doi.org/10.1017/aer.2016.66>
 28. Vuković J., Kos T. Augmentation of EGNOS ionospheric data with locally adapted ionospheric model. Poster presented at 11th European Space Weather Week, Liege, Belgium, November 17–21 2014.
 29. Ćwiklak J., Grzegorzewski M., Krasuski K. Influence of the Ionospheric Delay on Designation of an Aircraft Position. *Communications - Scientific Letters of the University of Zilina*. 2020, 22(3), 3–10, <https://doi.org/10.26552/com.C.2020.3.3-10>
 30. Grzegorzewski M., Świątek A., Ciećko A., Oszcza S., Ćwiklak J. Study of EGNOS safety of life service during the period of solar maximum activity. *Artificial Satellites*. 2012, 47, 137–145, <https://doi.org/10.2478/v10018-012-0019-5>
 31. Chaggara R., Paparini C., Ngayap-Youmbi U., Duparc B. In depth characterization of EGNOS ground stations response to space weather disturbances. *International Technical Symposium on Navigation and Timing (ITSNT) 2017*, 14–17 Nov 2017, ENAC, Toulouse, France, 1–7.
 32. Béniguel Y., Orus-Perez R., Prieto-Cerdeira R., Schlueter S., Scortan S., Grosu A. MONITOR 2: ionospheric monitoring network in support to SBAS and other GNSS and scientific purposes. 1–8, <https://ies2015.bc.edu/wp-content/uploads/2015/05/082-Beniguel-Paper.pdf>, (Accessed: 01.08.2023).
 33. Juan J. M., Sanz J., G. Gonzalez-Casado G., Rovira-Garcia A., Ibanez D., Orus R., Prieto-Cerdeira R., Schlüter S. Accurate reference ionospheric model for testing GNSS ionospheric correction in EGNOS and Galileo. 1–8, https://server.gage.upc.edu/papers/2014/73415_Juan.pdf, (Accessed: 01.08.2023).
 34. Schlüter S., Prieto-Cerdeira R., Orus R., Lam J. P., Juan Zornoza J. M. Sanz J., Hernández Pajares M. Characterization and modelling of the ionosphere for EGNOS development and qualification. A: The European Navigation Conference. In: *Proceedings of ENC 2013, Austria: 2013*, 1–5.
 35. IGS Technical Meeting 2004. Available from: http://ftp.aiub.unibe.ch/igs2004/Atmosphere_Ionosphere/FRAM1_Hernandez_1.pdf, (Accessed: 01.08.2023).
 36. Stankov S., Warnant R., Stegen K. Ionosphere effects on aviation, In: *Proceedings of the Eurocontrol LATO (Aircraft Landing and Take-Off) Work Group Meeting*, 7 July 2008, Toulouse, France, 1–17.
 37. Sauer K., Ochieng W.Y., Integrated use of GPS and EGNOS Carrier Phase Observations for High Precision Kinematic Positioning, In: *Proceedings of the 15th International Technical Meeting of the Satellite Division of The Institute of Navigation (ION GPS 2002)*, Portland, OR, September 2002, 914–920.
 38. Nie Z., Zhou P., Liu F., Wang Z., Gao Y. Evaluation

- of orbit, clock and ionospheric corrections from five currently available SBAS L1 services: methodology and analysis. *Remote Sens.* 2019, 11, 411, <https://doi.org/10.3390/rs11040411>
39. Pande A., Croitoru A., Ion M., Buehler S. RO-SISMON: Results and Multi-SBAS Fusion at user Level for Non-SoL Applications, In: *Proceedings of the 31st International Technical Meeting of the Satellite Division of The Institute of Navigation (ION GNSS+ 2018)*, Miami, Florida, September 2018, 1124–1143, <https://doi.org/10.33012/2018.15937>
 40. Tabti, L., Kahlouche, S., Benadda, B. Performance of the EGNOS system in Algeria for single and dual frequency. *International Journal of Aviation, Aeronautics, and Aerospace.* 2021, 8(3). <https://doi.org/10.58940/2374-6793.1622>
 41. Beldjilali B., Kahlouche S., Tabti L. Assessment of EGNOS performance for civil aviation flight phase in the edge coverage area. *Int. J. Aviat. Aeronaut. Aerosp.* 2020, 7, 1–25, <https://doi.org/10.15394/ijaaa.2020.1479>
 42. Volkov D. M., Zlunicyn O. I., Kocherova M. K., Talalaev A. B., Tikhonov V. V., Shishkovskaya K. G.. On a signal modeling technique for a back-inclined sensing in the multilayered ionosphere. *Vestnik TVGU. Ser. Prikl. Matem.* 2016, 2, 123–143.
 43. Sernov V. G., Isayev I. V., Filimonova D. V. A Method to calculate the ionospheric delay in ionospheric grid points in the wide-area functional augmentation of GLONASS. *Rocket-Space Device Engineering and Information Systems.* 2022, 9(2), 56–61, (in Russian).
 44. Lim C.-S., Byungwoon P., Hyoungmin S., Jaegy J., Seungwoo S., Junpyo P., Sung-Chun B., Chul-Soo L. Analysis on the multi-constellation SBAS performance of SDCM in Korea. *Journal of Positioning, Navigation, and Timing.* 2016, 5(4), 181–191, <https://doi.org/10.11003/JPNT.2016.5.4.181>
 45. Engineering statics website. Available from: <https://engineeringstatics.org/weghted-average.html>, (Accessed: 01.08.2023).
 46. Rovira-Garcia, A., Juan, J.M., Sanz, J. et al. Accuracy of ionospheric models used in GNSS and SBAS: methodology and analysis. *J. Geod.* 2016, 90, 229–240, <https://doi.org/10.1007/s00190-015-0868-3>
 47. Specht C., Pawelski J., Smolarek L., Specht M., Dabrowski P. Assessment of the positioning accuracy of DGPS and EGNOS systems in the bay of Gdansk using maritime Dynamic Measurements, *Journal of Navigation.* 2019, 72(3), 575–587, <https://doi.org/10.1017/s0373463318000838>
 48. Ciećko A., Bakula M., Grunwald G., Ćwiklak J. Examination of multi-receiver GPS/EGNOS positioning with kalman filtering and validation based on CORS stations. *Sensors.* 2020, 20, 2732, <https://doi.org/10.3390/s20092732>
 49. Kaniewski P. Joint processing of AHRS and GPS navigation data with kalman filter. *Biuletyn WAT.* 2006, 55(1), 271–284. (in Polish)
 50. Drony.net website. Available from: <https://www.drony.net/matrice-300-rtk-dji.html>, (Accessed: 01.08.2023).
 51. RTKLIB website. Available from: <http://rtklib.com/>, (Accessed: 01.08.2023).
 52. MAGNET Tools Website. Available from: <https://www.topconpositioning.com/office-software-and-services/survey-software/magnet-tools>, (Accessed: 01.08.2023).
 53. Scilab website. Available from: <https://www.scilab.org/>, (Accessed: 10.09.2022).
 54. Specht C., Mania M., Skóra M., Specht M. Accuracy of the GPS positioning system in the context of increasing the number of satellites in the constellation. *Polish Maritime Research.* 2015, 22, 9–14, <https://doi.org/10.1515/pomr-2015-0012>
 55. Bakota M., Kos S., Mrak Z., Brčić D. A new approach for improving GNSS geodetic position by reducing residual tropospheric error (RTE) based on surface meteorological data. *Remote Sens.* 2023, 15, 162, <https://doi.org/10.3390/rs15010162>
 56. Maciąg K., Maciąg M., Leń P. Implementation of unmanned aerial vehicles in the automated assessment of geodetic database validity. *Advances in Science and Technology Research Journal*, 2024, 18(7), 379–395.